A Power System Inertia Estimation Method Using Local Phasor Measurements from a Single Machine Considering Load Voltage Dependency

Yukai Wang, Jumpei Baba

***Abstract*—This paper proposes a novel method for power system inertia estimation using only local phasor measurements from a single machine, with consideration of load voltage dependency. The method begins by estimating the Center of Inertia (CoI) frequency based on local frequency measurements. It then fits the voltage dependency of loads using a linear approximation during the initial transient response following a disturbance. The effectiveness of the proposed approach is validated through simulations on the IEEE multi-machine test system under various conditions. Comparative analysis demonstrates the superiority of the proposed method over existing techniques, highlighting its accuracy and reduced complexity in estimating system inertia.**

***Keywords*—Center of Inertia Frequency, Inertia Estimation, Load Voltage Dependency, Local Phasor Measurements, Transient Response**

I. Introduction

POWER system inertia plays a key role in maintaining the stability of electrical grids, as it helps the system resist frequency deviations after disturbances. Traditionally, inertia is provided by the rotating masses of synchronous generators, which naturally respond to imbalances between supply and demand[1]. However, with the growing integration of renewable energy sources such as wind and solar power, which lack significant rotational inertia, the overall system inertia is decreasing [2]. This decline in inertia increases the system's vulnerability to frequency fluctuations, posing a greater risk of instability and outages [3].

As the energy landscape shifts, accurately estimating power system inertia has become essential for grid operators to ensure stable operation and develop effective control strategies.

Pioneering research in Japan during the late 20th century underscored the importance of quantifying power system inertia. Researchers developed a method to estimate inertia based on polynomial approximation of transient frequency changes caused by events such as generator outages or sudden load fluctuations[4]. While limited by measurement device constraints at the time, this early work laid the groundwork for subsequent advancements in inertia estimation.

Recently, the advent of high-precision synchrophasors or phasor measurement units (PMUs) has significantly transformed the landscape of power system inertia estimation. These devices enable synchronized measurements of phasors at various locations, providing high-fidelity data at microsecond timescales. This wealth of detailed information facilitates the development of more sophisticated transient data-based methods for inertia estimation.

With the advent of PMUs, research into inertia estimation has made significant strides. Adaptive polynomial fitting, as proposed in [5], optimizes the curve fit to transient frequency data.[6] focused on a narrower window for fitting and employed linear regression to reduce computational complexity [7] introduced a physical model-based approach, deriving differential equations to model transient frequency dynamics and enabling direct parameter estimation. [8] building upon the work in [7], incorporated the influence of the control system to enhance estimation accuracy. [9], [10], [11], [12] investigated the correlations between frequency and voltage variations during disturbances, modeling and calculating their effects using different segments of the disturbance process.[13], [14] proposed using sliding window averaging to mitigate the impact of sharp transient changes in the initial data. In addition,[15] contributed by fitting the system to a two-machine model through modal analysis, extracting inertia from the modal parameters.[16] accounted for the effects of primary frequency regulation by using a differential sampling window. [17], [18], [19] have employed various system identification algorithms and models to estimate inertia.

Despite the significant advancements in power system inertia estimation techniques, most existing methods rely on wide-area measurements or all available machine data, which can be costly, complex, and challenging to implement. These approaches often overlook the potential of localized measurements, which can offer faster, more accessible solutions in practical systems. Furthermore, the influence of load voltage dependency on system dynamics, particularly during transient conditions, remains underexplored in single-machine-based methods.

This study addresses these gaps by introducing a novel approach that enables inertia estimation using only local phasor measurements from a single machine, while incorporating load voltage dependency. The proposed method

This work was supported by JST SPRING, Grant Number JPMJSP2108.

Y. Wang is with the Department of Electrical Engineering and Information Systems, Graduate School of Engineering, The University of Tokyo, 7-3-1 Hongo, Bunkyo-ku, Tokyo 113-8656, Japan (e-mail: wangyukai@asc.t.u-tokyo.ac.jp).

J. Baba is with the Department of Advanced Energy, Graduate School of Frontier Sciences, The University of Tokyo, 7-3-1 Hongo, Bunkyo-ku, Tokyo 113-8656, Japan (e-mail: baba@asc.t.u-tokyo.ac.jp).

Paper submitted to the International Conference on Power Systems Transients (IPST2025) in Guadalajara, Mexico, June 8-12, 2025.

can achieve estimation within a short time after the disturbance event. By reducing the need for extensive measurement infrastructure, this method significantly lowers implementation complexity and enhances feasibility, making it particularly valuable for systems where only limited data is available. This innovation not only simplifies the estimation process but also expands the applicability of inertia estimation to a wider range of power systems, thereby providing a more efficient and scalable solution for maintaining grid stability.

The remainder of this paper is organized as follows: Section II introduces the theoretical foundations, including an overview of the swing equation and inflection point theory. Section III introduces the proposed methodology, outlining the process of estimating the COI frequency from single-machine frequency data using the inflection point theory and incorporating the voltage dependency of the load through single-machine voltage fitting. Section IV presents the test system utilized in this study. Section V provides a comprehensive evaluation of the proposed method using the IEEE 39-bus test system, including comparative analyses with existing methods. Section VI summarizes the key findings and conclusions of the study.

II. Theoretical Background

A. Swing Equation and system inertia

The stability and dynamic response of power systems are governed by the *swing equation*, which describes the rotor dynamics of synchronous machines in relation to the balance between mechanical power and electrical power. The swing equation formulation follows the classical derivation in [1], which is widely adopted for power system stability analysis. The swing equation, a second-order differential equation, represents the angular motion of the rotor and is expressed as:

$$2H\frac{d\Delta f}{dt} = \Delta P_m - \Delta P_e - D\Delta f \tag{1}$$

where H is the inertia constant of the generator, which is proportional to the mass and speed of the rotating parts, D is the damping coefficient, which is often neglected in dynamic analysis, Δf is the frequency deviation from which is equal to rotor angular speed in per unit value, Δf means the deviation from the nominal frequency, ΔP_m is the mechanical input power variation, and ΔP_e is the electrical output power variation.

This equation highlights the system's inertial response, as the difference between mechanical input and electrical output results in a change in the rotor angle, which subsequently affects system frequency. The rate of change of frequency (RoCoF) is directly related to the system inertia, with higher inertia providing a more gradual frequency response.

In a multi-machine system, the *Center of Inertia (CoI)* frequency represents the weighted average frequency of all the synchronous machines in the grid. It serves as a useful indicator for system-wide frequency behavior during disturbances. The CoI frequency, f_{CoI}, is defined as:

$$f_{\text{CoI}} = \frac{\sum_{i=1}^{n} H_i S_i f_i}{\sum_{i=1}^{n} H_i S_i} \tag{2}$$

where H_i is the inertia constant of machine i, f_i is the frequency of machine i, S_i is the capacity of machine i,and n is the total number of machines in the system.

The *system inertia*, H_{sys}, is the aggregate of the individual inertia constants of all connected machines and is calculated as:

$$H_{\text{sys}} = \frac{\sum_{i=1}^{n} H_i S_i}{S_{\text{base}}} \tag{3}$$

where S_i is the apparent power rating of machine i, and S_{base} is the system base power, which is typically $\sum_{i=1}^{n} S_i$.

This aggregated inertia reflects the system's ability to resist frequency changes during sudden disturbances. A higher H_{sys} indicates greater resistance to frequency deviations.

B. The Inflection Point Principle

As initially introduced in [20], the inflection point principle establishes a correlation between the local frequency curve and the COI frequency curve. This principle can be succinctly summarized by the following observation: during power imbalance disturbances, the response curves of the local frequency and COI frequency intersect at the inflection point of the local frequency curve, which corresponds to the point where the second derivative is zero.

It can be proved in the two-machine system as Fig.1.

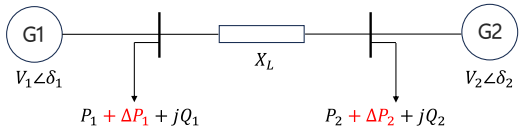

Fig. 1. Two-machine power system

Assuming that a power imbalance disturbance occurs in the system shown in Fig.1, the swing equations representing the two machines can be written as (4).

$$\begin{cases} 2H_1\dfrac{df_1(t)}{dt} = \Delta P_1 + \dfrac{V_1V_2}{X_L}\sin(\delta_1(t) - \delta_2(t)) \\ 2H_2\dfrac{df_2(t)}{dt} = \Delta P_2 - \dfrac{V_1V_2}{X_L}\sin(\delta_1(t) - \delta_2(t)) \end{cases} \tag{4}$$

Since $f = d\delta/dt$, derivation of the equations for t separately and collapsing it yields:

$$\begin{aligned} H_1\frac{d^2f_1(t)}{dt^2} &= -H_2\frac{d^2f_2(t)}{dt^2} \\ &= (f_1(t) - f_2(t))\frac{V_1V_2}{2X_L}cos(\delta_1(t) - \delta_2(t)) \end{aligned} \tag{5}$$

As demonstrated in the analysis, when the local frequencies of the two machines, $f_1(t) = f_2(t)$, the second-order derivative of the frequency, $d^2f(t)/dt^2$, becomes zero. This signifies the inflection point, where the frequency corresponds to the COI frequency. It is important to note that this principle has been refined in our previous research [21], as detailed in Section III.

III. Methodology

The proposed method is divided into two steps, the first step is to estimate the CoI frequency from local frequency measurements of a single machine using the inflection point principle, the second step is to approximate the equivalent CoI bus voltage from single machine terminal voltage measurements at the initial period, and hence the load voltage dependent variation, then the system inertia is estimated from them using the least squares method. The detailed process is described below.

A. CoI Frequency Estimation

Although [20] provides the inflection point principle which is helpful for extracting the COI component from local frequency, it does not give specific analysis, and its simple linear connection method is not suitable for quantitative calculations such as inertia estimation. Based on this, the authors have refined the principle in [21]. Please refer to the cited paper for details of the analysis, and a brief outline is presented here. Firstly, by decomposing the local frequency into the difference mode and common mode signals from the COI frequency, it is pointed out that the essence of the inflection point principle is to find the zero point of the difference mode signal. Since the difference mode signal is a decaying sinusoidal curve, its inflection point coincides with its zero point, so taking the inflection point can achieve the goal. However, the impact of load variations, particularly during the initial transient period, can distort the inflection point. To mitigate this, the initial inflection points, typically occurring before the first frequency extremum or within the first 0.5 seconds (for disturbances with a later extremum), are excluded. Subsequently, polynomial fitting is used to achieve the continuousness of the available discrete inflection points, as shown in (6) and (7).

$$\Delta F(t) = \frac{\sum_{i=0}^{n-1} a_{n-1,i} t^i + \sum_{i=0}^{n} a_{n,i} t^i + \sum_{i=0}^{n+1} a_{n+1,i} t^i}{3} \tag{6}$$

$$n = \left\lceil \frac{N}{2} \right\rceil \tag{7}$$

where $F(t)$ refers to the fitted frequency curve, a is the fitted polynomial coefficient, n is the median order of fitting polynomial, and N is the number of available inflection points. The equation represents the polynomial approximation of the fitted frequency $\Delta F(t)$. To account for potential randomness in the data, a median polynomial is obtained by averaging the results of three adjacent polynomial orders. Considering the trade-off between fast estimation and accuracy, 15 to 20 inflection points collected within 5 to 8 seconds are considered desirable[22].

B. Load Voltage Dependent Variation Approximation From Local Voltage

Previous studies often simplify the analysis by modeling the load as a constant power load, neglecting the impact of voltage variations. In contrast, this study explicitly incorporates the voltage dependency of the load, as described below.

Considering the system under the CoI model, which can be approximated as a single-unit, single-load system. When the system experiences a sudden load imbalance ΔP, a two-phase response mechanism emerges:

The initial phase is characterized by a rapid voltage change at the bus. This typically occurs within the first second following the disturbance, reflecting the system's natural response to the power imbalance. The rate and magnitude of this initial voltage change are primarily determined by the network parameters and the pre-disturbance operating conditions.

Following this initial phase, the system enters a recovery phase driven by the Automatic Voltage Regulator (AVR). The AVR system detects the voltage deviation and initiates corrective actions through the excitation system. This recovery process is notably slower than the initial change, typically spanning several seconds. This control action continues until the voltage approaches its nominal value.

Fig.2 illustrates the characteristic voltage response pattern when $\Delta P > 0$ as described above.

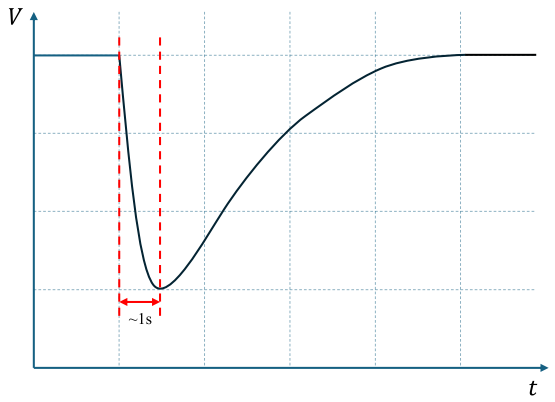

Fig. 2. Voltage Response to Power Imbalance Disturbance

In multi-machine power systems, the response mechanism becomes more complex but follows similar principles. When a load disturbance occurs, its impact is distributed among the participating generators based on their electrical proximity to the disturbance point and their relative strength in the network, quantified by their synchronizing coefficients. Each generator in the system experiences voltage variations that follow similar temporal patterns but with different magnitudes. Generators electrically closer to the disturbance point typically experience more pronounced voltage variations, while more distant units show attenuated responses. Despite these differences in magnitude, the temporal progression of voltage changes - from initial decline to AVR-driven recovery - remains consistent across all generators. Together, the responses of these generators form the response of the CoI bus equivalent voltage, as described below.

Based on the superposition principle and fundamental circuit theory, the voltage at any bus in the power system can be expressed as a linear combination of source voltages. This relationship still holds true for the virtual CoI bus.

The COI bus voltage can be mathematically expressed as:

$$V_{CoI} = \sum_{i=1}^{n} K_i V_i \tag{8}$$

In this expression, V_{CoI} is the voltage at the Center of Inertia bus, V_i represents the terminal voltage of the i-th generator, K_i denotes the participation factor of the i-th generator, and n is the total number of generators in the system. The participation factors K_i depend on the virtual electrical distance between the generator bus and the CoI bus.

To represent the CoI voltage using a single generator's voltage, we need to establish the relationships among different generator voltages. According to the previously discussed transient mechanism and voltage response curve, these relationships are inherently nonlinear and complex.

However, focusing on the initial response phase (typically within the first second after disturbance), we can exploit the rapid nature of the voltage changes to develop a simplified linear approximation. During this brief period, the voltage changes of the generator are considered to be linear with respect to time, and thus they are approximately constant in proportion to any another:

$$\frac{\Delta V_i(t)}{\Delta V_j(t)} \approx \alpha_{ij} \tag{9}$$

where α_{ij} is approximately constant during the initial stage, and $\Delta V_i(t)$, $\Delta V_j(t)$ are voltage changes relative to the pre-disturbance value.

This proportional relationship enables us to express any generator's voltage variation in terms of a reference generator (denoted as generator k):

$$\Delta V_i(t) = \alpha_{ik} \Delta V_k(t) \tag{10}$$

Substituting these relationships into the COI voltage equation:

$$\Delta V_{COI}(t) = \sum_{i=1}^{n} K_i \Delta V_i(t) = \sum_{i=1}^{n} K_i \alpha_{ik} \Delta V_k(t) \tag{11}$$

This can be simplified to:

$$\Delta V_{COI}(t) = \beta \Delta V_k(t) \tag{12}$$

where $\beta = (\sum_{i=1}^{n} K_i \alpha_{ik})$ is a constant determined by system conditions and reference generator location. Note that the above voltages are per unit values relative to the voltage during normal operation.

The approximation's validity is supported by the rapid nature of the initial response, during which slower dynamic processes have not yet significantly influenced the system's behavior.

The relationship between load power and voltage can be linearized around the equilibrium point using small-signal analysis. Consider a voltage-dependent load with power consumption $P_L(V)$.

Since the voltage variation is very small compared to the normal operation value, neglecting higher-order terms for small deviations and defining $\Delta V = V - V_0$, $\Delta P_L = P_L(V) - P_L(V_0)$, we obtain:

$$\Delta P_L = K_V P_0 \Delta V_{CoI} \tag{13}$$

where: $K_V = \frac{1}{P_0} \frac{\partial P_L}{\partial V}\big|_{V_0}$ is the voltage sensitivity coefficient of the load, and $P_0 = P_L(V_0)$ is the initial operating point power.

Combining this with our previous analysis of initial voltage response, and expressing ΔV in terms of a single reference generator voltage V_k:

$$\Delta P_L = K_V P_0 \beta \Delta V_k = P_0 \beta_{V,k} \Delta V_k \tag{14}$$

This linear relationship demonstrates that during the initial transient period, the load power variation can be represented as a function of a single generator's voltage deviation, scaled by the product of the load sensitivity coefficient, initial power, and the voltage distribution factor.

C. Single Machine Based System Inertia Estimation

According to (1), the swing equation under the CoI is:

$$2H \frac{d\Delta f_{CoI}}{dt} = \Delta P_m - \Delta P_e - D\Delta f_{CoI} \tag{15}$$

Given that the initial phase following a disturbance is of primary interest, and the frequency variation during this period is relatively small, the term associated with frequency variation can be neglected. Additionally, during this initial period, the mechanical power control system has not yet fully initiated its response. Furthermore, considering the power balance equation $\Delta P_e = \Delta P_L + P_d$, where P_d represents the load imbalance power which is usually known by the TSO. In practical implementations, P_d can be obtained through SCADA telemetry or predefined historical disturbance profiles. For instance, sudden load/generation changes are often associated with event-specific P_d values, which are cataloged by system operators. Then the swing equation can be expressed as:

$$2H \frac{d\Delta f_{CoI}}{dt} = -\Delta P_L - P_d \tag{16}$$

By substituting the estimated CoI frequency and voltage variations model into the equation, (17) is obtained:

$$2H \frac{d\Delta F_k(t)}{dt} = -P_0 \beta_{V,k} \Delta V_k(t) - P_d \tag{17}$$

where the subscript k represents the $k-$th generator. As observed, the equation contains two unknown variables: H and $\beta_{V,k}$. Using the measurement data collected during the initial post-disturbance period, we can establish an overdetermined system of equations to estimate H and $\beta_{V,k}$. Consider a series of measurements taken at time instances $t_1, t_2, ..., t_m$. At each time point, we have:

$$2H \frac{d\Delta F_k(t_i)}{dt} + P_0 \beta_{V,k} \Delta V_k(t_i) = -P_d \tag{18}$$

The solution is given by:

$$\mathbf{Ax} = \mathbf{b} \tag{19}$$

where $\mathbf{x} = [2H, \beta_{V,k}]^T$ is the parameter vector to be estimated. And:

$$\mathbf{A} = \begin{bmatrix} \frac{d\Delta F_k(t_1)}{dt} & P_0\Delta V_k(t_1) \\ \frac{d\Delta F_k(t_2)}{dt} & P_0\Delta V_k(t_2) \\ \vdots & \vdots \\ \frac{d\Delta F_k(t_m)}{dt} & P_0\Delta V_k(t_m) \end{bmatrix} \mathbf{b} = \begin{bmatrix} -P_d \\ -P_d \\ \vdots \\ -P_d \end{bmatrix} \tag{20}$$

The least squares solution for the unknown parameters can then be obtained by:

$$\begin{bmatrix} 2\hat{H} \\ \hat{\beta}_{V,k} \end{bmatrix} = (\mathbf{A}^T\mathbf{A})^{-1}\mathbf{A}^T\mathbf{b} \tag{21}$$

IV. Test System

To evaluate the effectiveness of the proposed inertia estimation method, simulations were conducted using the IEEE New England 10-machine, 39-bus test system, modeled in MATLAB/Simulink. This test system is widely used for power system stability analysis due to its complexity and realistic representation of an interconnected network. The system consists of 10 synchronous generators and 39 buses, along with various loads and transmission lines, allowing for comprehensive testing of dynamic behavior under different disturbance scenarios.

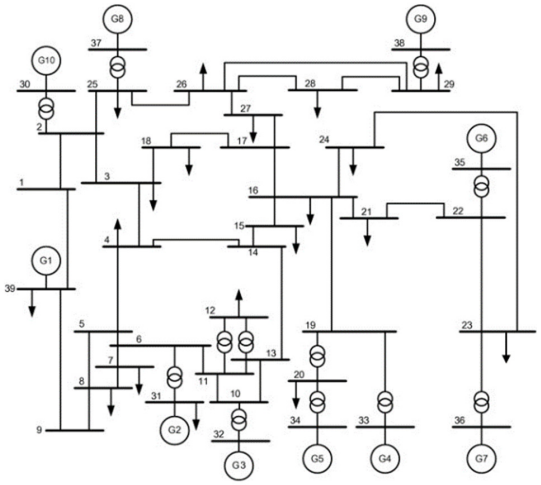

Fig. 3. IEEE New England 10-machine 39-bus test system

To accurately represent the behavior of an actual power system, the simulation model incorporates detailed representations of system components. Synchronous generators are modeled using a comprehensive seventh-order model. The control systems include IEEE Type 1 governors and multi-band power system stabilizers for each generator, as outlined in [23]. Generators 3, 6, and 9 are specifically modeled as hydro turbine-governor systems, while G8 is represented as a Virtual Synchronous Generator (VSG), following the approaches described in [24], [25], [26]. The VSGs emulate the external characteristics of traditional synchronous generators, which reflects the current and near-future power systems where synchronous generators remain dominant. On the other hand, non-responsive renewable energy sources are modeled as constant generation sources or integrated into constant power loads. The remaining generators utilize steam turbine-governor systems. Load models are implemented using the ZIP model. The PMU sampling rate is set to 100 Hz. The inertia distribution data for the system is provided in the Table I.

TABLE I
System Inertia Distribution

Gen No.	1	2	3	4	5	6	7	8	9	10	Sys
Base MVA	1000	1000	1000	1000	1000	1000	1000	1000	1000	1000	10000
H	7.04	3.03	3.58	2.86	2.60	3.48	2.64	2.83	3.45	4.2	3.531

V. Case Study

To validate the effectiveness of the proposed method, a case study is conducted on the previously introduced IEEE test system. Given the lack of existing methods for estimating system inertia using purely local measurements, we select two comparative methods for this evaluation. The first comparative method (Compared Method 1) is a simplified version of the proposed method that ignores load voltage dependency, to highlight the impact of incorporating voltage dependency in inertia estimation. The second comparison (Compared Method 2) employs the method outlined in [27], which estimates the power imbalance by utilizing the linear component of local frequency measurements. This method can also estimate inertia when the power imbalance is known, making it suitable for comparison with the proposed method due to its similar application conditions.

As the first test case, a 600 MW (0.06 p.u.) load increase is introduced at bus 15. The system load composition is assumed to follow a ratio of $Z : I : P = 3 : 3 : 4$, representing the proportions of constant impedance, constant current, and constant power loads, respectively. Additionally, the damping coefficient D is set to 1. For the estimation of the CoI frequency, 15 inflection points are used. The time window for inertia estimation is set to within the first 0.5 seconds after the disturbance. The test results using measurements from each single machine are presented in Table II, where the estimates and relative errors are listed.

TABLE II
Estimation Results using tested methods for Case 1

	Proposed Method			Compared Method 1		Compared Method 2	
Gen No.	$\hat{H}$	ϵ_H	β_V	$\hat{H}$	ϵ_H	$\hat{H}$	ϵ_H
G1	3.8660	9.49%	1.50	5.4389	54.03%	5.3625	51.87%
G2	3.7274	5.56%	0.97	6.0325	70.85%	6.0680	71.85%
G3	3.9531	11.96%	0.85	5.8920	66.86%	5.9166	67.56%
G4	3.7774	6.98%	0.81	6.2256	76.31%	5.7641	63.24%
G5	3.5403	0.26%	0.79	5.8882	66.76%	6.5042	84.20%
G6	3.6007	1.97%	0.94	5.9934	69.74%	5.4489	54.32%
G7	3.8663	9.50%	0.99	6.3008	78.44%	5.7597	63.12%
G8	3.9322	11.36%	0.90	6.6104	87.21%	7.4309	110.45%
G9	3.4184	-3.19%	1.02	5.5592	57.44%	7.4416	110.75%
G10	3.4415	-2.53%	1.35	5.4270	53.69%	5.3694	52.06%

The proposed method demonstrates higher accuracy in estimating inertia compared to the two benchmark methods,

producing values that are closer to the actual system inertia. This improvement is reflected in the significantly smaller relative errors under various conditions, highlighting the advantage of considering the voltage dependency. The variation in estimation errors across reference generators stems from unavoidable CoI frequency estimation inaccuracies and inflection point distribution uncertainties. By incorporating voltage sensitivity through the coefficient β_V, the proposed method can dynamically adjust its estimates based on the observed voltage response, thereby providing a more detailed and accurate understanding of the system inertia behavior.

In contrast, the Compared Method 1, which does not consider voltage variations, exhibits larger estimation errors. This difference highlights the importance of incorporating voltage dynamics into inertia estimation, especially in systems where load composition is related to voltage. Compared Method 2 relies on the linear component of the local frequency to estimate power imbalance, and its derivation is also obtained by ignoring the load voltage-dependent variation. Therefore, this method also shows limitations in this case, leading to relatively high errors.

As an illustration, Fig.4 presents the estimated CoI frequency results based on G2, where the f_{poly} means the estimated CoI frequency.

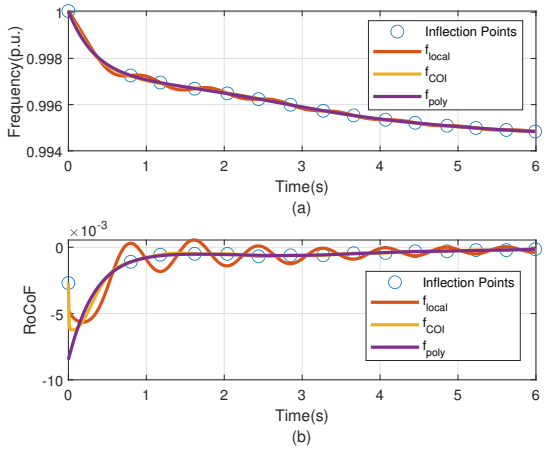

Fig. 4. Estimated CoI frequency and RoCoF based on G2 measurements

To investigate the performance of considering load voltage variations in the proposed method, the load variations calculated using the coefficient β_V and single machine voltage are plotted on the same figure as the load variations calculated using the total generator output, as shown in Fig.5.

The ΔP_o indicates the load variation calculated using the system's generation output. It can be seen that the compliance variations calculated using the load-voltage coefficients of the proposed methodology are very close to the actual load variations, which also shows the validity of the proposed methodology.

To further assess the generality and scalability of the proposed method, additional simulations are conducted under three modified system conditions, with all other parameters remaining constant unless explicitly stated.

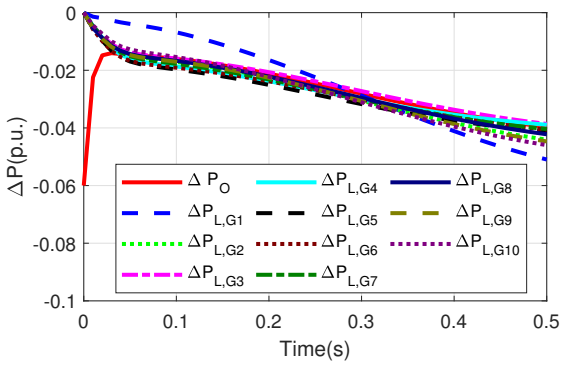

Fig. 5. Load power variation calculated using single machine data and outputs

- **Case 2**: G8 is replaced by renewable source generation without inertia support, resulting in a reduced system inertia of 3.248 s, load ratio $Z : I : P = 2 : 3 : 5$; 700 MW(0.07 p.u.) load increase at bus 27.
- **Case 3**: All generators' inertia is reduced by 30%, leading to a system inertia of 2.472 s, load ratio $Z : I : P = 2 : 2 : 6$; 600 MW(0.06 p.u.) load increase at bus 16.
- **Case 4**:All generators' inertia is increased by 30%, leading to a system inertia of 4.590 s, load ratio $Z : I : P = 1 : 1 : 8$; 500 MW(0.05 p.u.) load decrease at bus 3.

TABLE III
ESTIMATION RESULTS USING TESTED METHODS FOR CASE 2

	Proposed Method			Compared Method 1		Compared Method 2	
Gen No.	$\hat{H}$	ϵ_H	β_V	$\hat{H}$	ϵ_H	$\hat{H}$	ϵ_H
G1	3.5582	8.22%	1.23	4.9591	50.82%	4.6859	42.51%
G2	3.1512	-4.16%	0.87	5.0185	52.63%	6.0500	84.00%
G3	3.1296	-4.82%	0.87	4.9934	51.87%	6.0174	83.01%
G4	3.5366	7.56%	0.69	5.5510	68.83%	5.8015	76.45%
G5	2.9852	-9.21%	0.74	4.7520	44.52%	7.2720	121.17%
G6	3.1051	-5.56%	0.87	5.1078	55.35%	5.6398	71.53%
G7	3.2921	0.13%	0.95	5.3865	63.82%	5.8073	76.62%
G9	3.1881	-3.04%	0.62	5.4164	64.73%	5.1665	57.13%
G10	3.4276	4.24%	1.04	5.4893	66.95%	4.8163	46.48%

TABLE IV
ESTIMATION RESULTS USING TESTED METHODS FOR CASE 3

	Proposed Method			Compared Method 1		Compared Method 2	
Gen No.	$\hat{H}$	ϵ_H	β_V	$\hat{H}$	ϵ_H	$\hat{H}$	ϵ_H
G1	2.4240	-1.93%	1.03	3.2690	32.26%	3.3654	36.16%
G2	2.4167	-2.23%	0.69	3.6160	46.29%	4.0295	63.03%
G3	2.3244	-5.96%	0.72	3.5470	43.50%	4.1481	67.83%
G4	2.4624	-0.37%	0.59	3.8947	57.57%	3.7796	52.92%
G5	2.8279	14.41%	0.40	4.2557	72.18%	4.1785	69.06%
G6	2.4851	0.54 %	0.65	3.8664	56.43%	3.6309	46.90%
G7	2.5223	2.05%	0.70	4.0686	64.61%	3.9606	60.24%
G8	2.6371	6.69%	0.66	4.0635	64.40%	4.7967	94.06%
G9	2.7393	10.83%	0.58	4.0158	62.47%	4.6535	88.27%
G10	2.5458	3.00 %	0.93	3.8129	54.26%	3.4641	40.15%

The simulation results across various test cases demonstrate the effectiveness of the proposed inertia estimation method, particularly when compared to the methods that disregard load voltage dependency. In each case, the proposed method consistently produced inertia estimates with lower relative

TABLE V
ESTIMATION RESULTS USING TESTED METHODS FOR CASE 4

	Proposed Method			Compared Method 1		Compared Method 2	
Gen No.	$\hat{H}$	ϵ_H	β_V	$\hat{H}$	ϵ_H	$\hat{H}$	ϵ_H
G1	4.9381	7.58%	0.18	5.2080	13.46%	4.4452	-3.16%
G2	4.3857	-4.46%	0.46	5.3625	16.82%	5.8940	28.40%
G3	4.4714	-2.59%	0.44	5.3996	17.63%	5.6380	22.82%
G4	4.7575	3.64%	0.37	5.5635	21.20%	6.1487	33.95%
G5	4.1779	-8.98%	0.51	5.3212	15.92%	7.1953	56.75%
G6	4.9635	8.13%	0.37	5.6973	24.12%	5.8302	27.01%
G7	5.2282	13.90%	0.34	5.8828	28.16%	6.1236	33.40%
G8	5.0931	10.95%	0.40	6.0893	32.66%	6.0646	32.12%
G9	4.9002	6.75%	0.32	5.6565	23.23%	6.2850	36.92%
G10	4.4632	-2.77%	0.52	5.4070	17.79%	4.5254	-1.41%

error. This advantage is primarily due to the integration of load voltage dependency, which provides a more accurate representation of system dynamics following disturbances.

The comparative analysis highlights that neglecting load voltage dynamics, as in Compared Method 1, leads to substantial errors, especially in cases where load composition is closely related to voltage, such as in modern grids with complex, responsive loads. Similarly, the limitations of Compared Method 2, which relies solely on local frequency data without accounting for voltage dependency, reinforce the necessity of our approach in accurately capturing the transient response. From the tabulated results, it is also evident that the compared methods, tend to yield higher accuracy in cases where load voltage dependency variations are minimal. On the other hand, this further highlights their limitations.

In scenarios with modified system conditions, the proposed method demonstrated robustness. These cases underscore the scalability of the method, confirming its adaptability across different power systems and conditions. In particular, Case 2 and Case 3 revealed that even with significant reductions in system inertia, our approach maintained accuracy, suggesting its potential applicability for future low-inertia grids.

Furthermore, in comparison with the reported precision of mainstream wide-area measurement-based methods, the proposed method shows no inferiority, achieving comparable accuracy without requiring extensive measurement infrastructure. This capability makes it a practical alternative for systems with limited PMU distribution.

VI. CONCLUSIONS

This study presents a novel method for estimating power system inertia using local phasor measurements from a single machine, incorporating load voltage dependency. The proposed method addresses the challenge in conventional inertia estimation approaches that rely on system-wide, wide-area measurements. Through case studies on the IEEE 39-bus test system, this method demonstrates improved accuracy, particularly in scenarios with significant load voltage dependency, by dynamically adapting inertia estimates based on voltage response. This innovation provides a practical and efficient solution for inertia estimation, supporting stability in low-inertia power systems. What's more, the proposed method offers a viable solution for systems with limited PMU distribution.

Future work could involve testing the method with real-world data, improving CoI frequency estimation accuracy, extending the approach to interconnected multi-area systems, integrating inertia estimation with other frequency response parameters for comprehensive stability analysis, and the additional considerations for stability evaluation of IBR(Inverter Based Resource)-dominated grids with the higher flexibility and faster dynamics. Future work will also explore the integration of artificial intelligence techniques to estimate inertia under conditions where the disturbance magnitude P_d is unknown.

REFERENCES

[1] P. Kundur, *Power System Stability and Control*. New York: McGraw-hill, 1994.

[2] A. Fernández-Guillamón, E. Gómez-Lázaro, E. Muljadi, and Á. Molina-García, "Power systems with high renewable energy sources: A review of inertia and frequency control strategies over time," *Renewable and Sustainable Energy Reviews*, vol. 115, p. 109369, Nov 2019.

[3] C. Agathokleous and J. Ehnberg, "A quantitative study on the requirement for additional inertia in the european power system until 2050 and the potential role of wind power," *Energies*, vol. 13, no. 9, 2020.

[4] T. Inoue, H. Taniguchi, Y. Ikeguchi, and K. Yoshida, "Estimation of Power System Inertia Constant and Capacity of Spinning-reserve Support Generators Using Measured Frequency Transients," *IEEE Transactions on Power Systems*, vol. 12, no. 1, pp. 136–143, 1997.

[5] C. Phurailatpam, Z. H. Rather, B. Bahrani, and S. Doolla, "Measurement-Based Estimation of Inertia in AC Microgrids," *IEEE Transactions on Sustainable Energy*, vol. 11, no. 3, pp. 1975–1984, Jul 2020.

[6] M. Sun, Y. Feng, P. Wall, S. Azizi, J. Yu, and V. Terzija, "On-line power system inertia calculation using wide area measurements," *International Journal of Electrical Power and Energy Systems*, vol. 109, no. November 2018, pp. 325–331, Jul 2019.

[7] R. K. Panda, A. Mohapatra, and S. C. Srivastava, "Online Estimation of System Inertia in a Power Network Utilizing Synchrophasor Measurements," *IEEE Transactions on Power Systems*, vol. 35, no. 4, pp. 3122–3132, 2020.

[8] S.-h. Lee, J.-h. Liu, B.-y. Chen, and C.-c. Chu, "A Two-Stage Data-Driven Method for Estimating the System Inertia Utilizing Event-Driven PMU Measurements," *IEEE Transactions on Industry Applications*, vol. 59, no. 5, pp. 5243–5256, Sep 2023.

[9] D. Zografos and M. Ghandhari, "Estimation of power system inertia," in *2016 IEEE Power and Energy Society General Meeting*, Jul 2016, pp. 1–5.

[10] D. Zografos, M. Ghandhari, and K. Paridari, "Estimation of power system inertia using particle swarm optimization," in *2017 19th International Conference on Intelligent System Application to Power Systems (ISAP)*, Sep 2017, pp. 1–6.

[11] D. Zografos and M. Ghandhari, "Power system inertia estimation by approaching load power change after a disturbance," in *2017 IEEE Power and Energy Society General Meeting*, Jul 2017, pp. 1–5.

[12] D. Zografos, M. Ghandhari, and R. Eriksson, "Power system inertia estimation: Utilization of frequency and voltage response after a disturbance," *Electric Power Systems Research*, vol. 161, pp. 52–60, 2018.

[13] P. Wall, F. Gonzalez-Longatt, and V. Terzija, "Estimation of generator inertia available during a disturbance," in *2012 IEEE Power and Energy Society General Meeting*, Jul 2012, pp. 1–8.

[14] P. Wall and V. Terzija, "Simultaneous estimation of the time of disturbance and inertia in power systems," *IEEE Transactions on Power Delivery*, vol. 29, no. 4, pp. 2018–2031, 2014.

[15] G. Cai, B. Wang, D. Yang, Z. Sun, and L. Wang, "Inertia Estimation Based on Observed Electromechanical Oscillation Response for Power Systems," *IEEE Transactions on Power Systems*, vol. 34, no. 6, pp. 4291–4299, 2019.

[16] Y. Wang, A. Yokoyama, and J. Baba, "A Multifunctional Online Estimation Method for Synchronous Inertia of Power Systems Using Short-Time Phasor Transient Measurement Data With Linear Least Square Method After Disturbance," *IEEE Access*, vol. 12, no. January, pp. 17 010–17 022, 2024.

[17] F. Zeng, J. Zhang, G. Chen, Z. Wu, S. Huang, and Y. Liang, "Online Estimation of Power System Inertia Constant under Normal Operating Conditions," *IEEE Access*, vol. 8, pp. 101 426–101 436, 2020.
[18] P. Makolo, I. Oladeji, R. Zamora, and T. T. Lie, "Data-driven inertia estimation based on frequency gradient for power systems with high penetration of renewable energy sources," *Electric Power Systems Research*, vol. 195, no. September 2020, p. 107171, 2021.
[19] S. C. Dimoulias, E. O. Kontis, and G. K. Papagiannis, "On-line tracking of inertia constants using ambient measurements," *Electric Power Systems Research*, vol. 224, no. March, p. 109643, nov 2023.
[20] S. Azizi, M. Sun, G. Liu, and V. Terzija, "Local Frequency-Based Estimation of the Rate of Change of Frequency of the Center of Inertia," *IEEE Transactions on Power Systems*, vol. 35, no. 6, pp. 4948–4951, Nov 2020.
[21] Y. Wang and J. Baba, "An Inflection Point Polynomial Fitting Based Estimation Method for Center of Inertia Frequency and Its Rates of Change Using Single Machine Measurements," in *2024 IEEE Power and Energy Society General Meeting*, Jul 2024.
[22] Y. Wang and J. Baba, "Leveraging Simulation-Based Statistical Analysis for Optimal Polynomial and Inflection Point Selection in Local Frequency-Based Center of Inertia Frequency Estimation," in *2024 3rd International Conference on Power Systems and Electrical Technology (PSET)*, Aug 2024.
[23] IEEE Recommended Practice for Excitation System Models for Power System Stability Studies, *IEEE Std 421.5-2016*. IEEE, 2016.
[24] W. G. P. Mover and E. Supply, "Hydraulic turbine and turbine control models for system dynamic studies," *IEEE Transactions on Power Systems*, vol. 7, no. 1, pp. 167–179, 1992.
[25] IEEE Report, "Dynamic Models for Steam and Hydro Turbines in Power System Studies," *IEEE Transactions on Power Apparatus and Systems*, vol. PAS-92, no. 6, pp. 1904–1915, Nov 1973.
[26] J. Alipoor, Y. Miura, and T. Ise, "Power System Stabilization Using Virtual Synchronous Generator With Alternating Moment of Inertia," *IEEE Journal of Emerging and Selected Topics in Power Electronics*, vol. 3, no. 2, pp. 451–458, Jun 2015.
[27] J. Li, Y. Li, W. Li, S. Yang, and Z. Du, "System Power Imbalance Estimation Utilizing Linear Component of Local Frequency," *IEEE Transactions on Power Systems*, vol. 39, no. 1, pp. 2373–2376, Jan 2024.